Research Square

Preprints are preliminary reports that have not undergone peer review.
They should not be considered conclusive, used to inform clinical practice,
or referenced by the media as validated information.

# GPR15LG selectively amplifies stimulus-induced responses of human immune cells and restricts M2-associated macrophage polarization

**Sofya Albers**
Ulm University Medical Centre
**Lara Fielitz**
Ulm University Medical Centre
**Dan Albers**
Ulm University Medical Centre
**Florian Klassen**
Ulm University Medical Centre
**Tobias Nüssle**
Ulm University Medical Centre
**Sabine Vettorazzi**
Ulm University
**Jan Münch**
Ulm University Medical Centre
**Mirja Harms**
Mirja.harms@uni-ulm.de

Ulm University Medical Centre

**Research Article**

**Keywords:** GPR15LG, monocytes, macrophage polarization, inflammation, Toll-like receptor 4

**Posted Date:** November 26th, 2026

**DOI:** https://doi.org/10.21203/rs.3.rs-11550847/v1

**License:** This work is licensed under a Creative Commons Attribution 4.0 International License.
Read Full License

**Additional Declarations:** No competing interests reported.

## Abstract

# Background

GPR15LG is a cationic, chemokine-like peptide that is induced at inflamed epithelial barriers. Whether it modulates human immune-cell activation beyond its established role in chemotaxis is unknown.

# Methods

PBMCs, enriched NK cells, monocytes and monocyte-derived macrophages from healthy adult blood donors (n = 3–8 per experiment) and THP-1 reporter cells were exposed to full-length GPR15LG (0.03–5 μM) or its N-terminal (aa 25–41) or C-terminal (aa 58–84) fragments, with or without CD3/CD28 stimulation, CXCL12, polarizing cytokines or TLR agonists. Readouts included transwell migration, multiplex cytokine assays, flow cytometry, supernatant transfer, live-cell phagocytosis imaging and NF-κB/AP-1 reporter assays.

# Results

GPR15LG alone induced little cytokine release but, during CD3/CD28 stimulation, selectively increased IFN-γ, IFN-α2, IL-18, IL-6, IL-10, CCL2 and CXCL8. NK-cell activation rose indirectly, via conditioned supernatants, without increased cytotoxicity. GPR15LG raised monocyte CD80, restricted acquisition of a CD80 − CD163+ phenotype during IL-4 polarization and lowered phagocytic capacity of the resulting macrophages, whereas acute exposure did not. Activity required the full-length peptide and potentiated LPS-induced, TLR4-dependent responses.

# Conclusion

GPR15LG is not an autonomous immune activator but a selective amplifier of ongoing inflammatory responses that also redirects macrophage polarization. The mediating receptor remains unidentified.

## 1 Introduction

GPR15LG (GPR15 ligand), also known as GPR15L, C10orf99 or AP-57, is a highly cationic, chemokine-like protein predominantly expressed at epithelial barrier tissues [1]. GPR15LG is constitutively abundant in the gastrointestinal mucosa and can be strongly induced in inflamed skin, including in psoriasis and atopic dermatitis [2, 3]. Initially described as an antimicrobial peptide, GPR15LG was subsequently identified as the endogenous ligand of the G protein-coupled receptor GPR15, thereby establishing a role for the protein in immune-cell trafficking [1, 4]. Through GPR15, GPR15LG promotes the recruitment of GPR15-expressing lymphocyte populations and has been implicated in T-cell homing to epithelial tissues, particularly the large intestine and skin [4–6]. Beyond this canonical receptor-ligand interaction,

accumulating evidence indicates that GPR15LG exerts additional, partly GPR15-independent functions in epithelial homeostasis and inflammation [7, 8].

We recently identified the chemokine receptor CXCR4 as an additional receptor for GPR15LG and demonstrated that GPR15LG modulates CXCR4 signaling in a context-dependent manner [9]. In particular, when GPR15LG and the endogenous CXCR4 ligand CXCL12 are presented simultaneously, GPR15LG strongly potentiates CXCL12-induced signaling and migration of primary human immune cells, including CD4 + T cells [9]. Thus, GPR15LG can modulate immune-cell trafficking independently of its canonical interaction with GPR15 and may influence the recruitment of immune cells into CXCL12-rich inflammatory tissues.

Immune-cell recruitment represents only the initial phase of a tissue immune response. Once recruited to inflamed tissues, lymphoid and myeloid cells encounter combinations of cytokines, chemokines and microbial or damage-associated signals that determine their subsequent activation and functional state [10–12]. At barrier sites this includes continuous engagement of pattern-recognition receptors: epithelial injury and microbial exposure activate Toll-like receptors (TLRs) on infiltrating myeloid cells, while the local cytokine milieu simultaneously directs monocyte-to-macrophage differentiation and polarization towards inflammatory or resolution-associated states. In addition, host-defense peptides can modulate such responses. An example is the Cathelicidin LL-37, a cationic peptide which modulates pattern-recognition receptor activity by binding their ligands thereby altering ligand stability, cellular uptake and receptor engagement. [13–15]. GPR15LG is comparably cationic and is co-induced with cathelicidins at inflamed epithelial sites. Whether GPR15LG likewise modulates TLR-dependent activation of myeloid cells is unexplored. We hypothesized that the biological activity of GPR15LG may extend beyond the regulation of cellular migration and influence how recruited immune cells respond to activating signals.

Here, we investigated the effects of GPR15LG on human lymphoid and myeloid immune-cell responses. We first examined whether its previously identified enhancement of CXCL12-dependent migration is maintained in activated T cells and subsequently assessed its impact on immune activation in stimulated PBMCs. We then investigated GPR15LG-mediated effects on NK cells and monocytes and determined whether prolonged exposure alters macrophage differentiation, polarization and phagocytic function. Finally, using GPR15LG-derived peptide fragments, defined Toll-like receptor stimuli, pharmacological inhibition and reporter cells, we explored structural and signaling requirements underlying its immunomodulatory activity. Our findings identify GPR15LG as a context-dependent modulator that links immune-cell trafficking with the selective amplification and redirection of innate immune responses. Because the receptor requirements of this activity are not known, we present the study as a systematic characterization of GPR15LG activity on human immune cells and state explicitly, for each observation, whether the effect is direct, indirect or mechanistically unassigned.

# 2 Materials and Methods

**Reagents**. Full-length human GPR15LG was custom synthesized by Bachem. The identity and purity of the peptide were confirmed by the manufacturer, and the corresponding certificates of analysis are provided in the Supplementary Material. Peptide purity was ≥ 92% as determined by reversed-phase HPLC, and peptide identity was confirmed by MALDI-TOF mass spectrometry (observed m/z 6516.0). The N-terminal (aa 25–41) and C-terminal (aa 58–84) fragments were produced using identical solid-phase synthesis, purification and handling procedures. Lyophilized peptides were reconstituted in PBS. The TLR4 antagonist resatorvid (TAK-242) was obtained from Selleckchem. The TLR2 antagonist MMG-11 was obtained from MedChemExpress. Stock solutions were prepared in DMSO or endotoxin-free water (for PAM3CSK4) and stored at -20°C. Corresponding vehicle controls were included in all experiments. Recombinant human IL-2, IL-15 and IL-12 were obtained from Miltenyi Biotec. Recombinant human M-CSF, CXCL12/SDF-1α, IFN-β, and IFN-γ were obtained from PeproTech. Recombinant human IL-4 and IL-18 were obtained from R&D Systems. Lipopolysaccharide from Escherichia coli was obtained from Sigma-Aldrich. The TLR7/8 agonist R848 and TLR2 agonist PAM3CSK4 were obtained from InvivoGen.

**Cell lines and culture conditions.** THP-1 and K562 cells were obtained from ATCC. THP1-Dual cells carrying secreted NF-κB/AP-1 and IRF reporter systems were obtained from InvivoGen. Cells were cultured in complete RPMI-1640 medium containing 10% fetal calf serum, 1% penicillin/streptomycin and 1% L-glutamine at 37°C in a humidified atmosphere containing 5% $CO_2$. THP1-Dual cells were maintained in the presence of the recommended selection antibiotic Zeocin according to the manufacturer's instructions.

**Isolation and culture of primary human cells.** Peripheral blood mononuclear cells (PBMCs) were isolated from citrate-anticoagulated buffy coats obtained from healthy adult donors by Ficoll density-gradient centrifugation. Use of buffy coats from healthy, anonymized blood donors did not require separate approval by the Ethics Committee of Ulm University; all donors provided written informed consent. Residual erythrocytes were removed by incubation with ACK lysis buffer (Lonza) for 5 min at room temperature. Following lysis, PBMCs were washed and cultured in complete RPMI-1640 medium as described above. CD4 + T cells used in migration experiments were isolated from PBMCs using the RosetteSep™ Human CD4 + T Cell Enrichment Cocktail (STEMCELL Technologies). The purity of the isolated population was over 95%, as assessed by flow cytometry. NK cells were enriched using the RosetteSep Human NK Cell Enrichment Cocktail (STEMCELL Technologies) according to the manufacturer's instructions. Enriched cells were rested for up to 3 days in NK MACS Medium supplemented with 1× NK MACS Supplement (Miltenyi Biotec) and 5% human AB serum at 37°C and 5% $CO_2$. The proportion of CD3 − CD56+ NK cells in the enriched populations ranged from 60% to 80%, as determined by flow cytometry. Accordingly, these preparations are referred to as NK-cell-enriched rather than purified NK-cell populations. Monocytes were isolated using the EasySep Human Monocyte Enrichment Kit without CD16 depletion (STEMCELL Technologies), according to the manufacturer's instructions. Enriched monocytes were used directly for macrophage differentiation. Monocyte purity was assessed by flow cytometry and was between 60–80%.

**Transwell migration assay.** Migration assays were performed as described in details by Albers et al. [9].

**PBMC stimulation.** Flat-bottom 96-well plates were coated with 65 µL per well of anti-CD3 antibody (clone OKT3, Invitrogen) at the indicated concentrations for 3 h at 37°C and washed twice with PBS. PBMCs (150,000 per well) were added in serum-free X-VIVO 15 medium (Lonza) with 1% penicillin/streptomycin and 1% L-glutamine. Where applicable, cells were preincubated for 15 min with the TLR4 antagonist resatorvid or the TLR2 antagonist MMG-11, and then for a further 15 min with GPR15LG or vehicle. Soluble anti-CD28 antibody (BioLegend, 5 µg/mL) and 50 U/mL IL-2 were then added, and cells were incubated as indicated before flow cytometry or supernatant collection. For TLR4-driven stimulation 1 ng/mL LPS was added to cells in the absence or presence of GPR15LG; untreated cells and stimulus-only conditions (without GPR15LG) served as controls. Cells were incubated for 24 h before flow-cytometric analysis of CD80 surface expression.

**NK cell stimulation.** NK-cell-enriched preparations were seeded in V-bottom plates at a final density of $7.5 \times 10^5$ cells/mL in X-VIVO 15 medium supplemented with 1% penicillin/streptomycin and 1% L-glutamine. Cells were stimulated for 72 h with the indicated concentrations of IL-2, IL-12, IL-15 or IL-18 in the presence or absence of 1 µM GPR15LG, unless otherwise indicated. Cells were subsequently collected and analyzed by flow cytometry.

**Supernatant-transfer assay.** PBMCs were stimulated with plate-bound anti-CD3 and soluble anti-CD28 in the presence or absence of GPR15LG as described above. After 24 hours, culture supernatants were collected by centrifugation at 300xg for 3 minutes and transferred to NK-cell-enriched cultures so that conditioned PBMC supernatant constituted 87.5% of the final recipient culture volume. Where indicated, GPR15LG was also added directly to the recipient culture; these conditions distinguish effects transferred with the supernatant from effects of peptide addition to recipient cells. Recipient cells were incubated for 24 hours before CD69 and CD107a expression was assessed by flow cytometry.

**TLR stimulation of THP-1 cells.** THP-1 cells were seeded at $1 \times 10^5$ cells per well in a 96-well plate. Cells were preincubated with 5 µM GPR15LG or vehicle for 15 min before stimulation for indicated times with the indicated concentrations of LPS, R848 or PAM3CSK4, which were used as agonists of TLR4, TLR7/8 and TLR2, respectively. Following stimulation, activation was assessed by flow cytometry.

**NF-κB/AP-1 and IRF reporter assays**. THP1-Dual cells were seeded at 100 000 cells per well in a 96-well plate and preincubated with GPR15LG or the corresponding vehicle controls as described above. Cells were subsequently stimulated with the indicated TLR agonists for 24 hours. NF-κB/AP-1-dependent secreted embryonic alkaline phosphatase activity was quantified in cell-culture supernatants using the QuantiBlue Solution according to the manufacturer's instructions. Absorbance was measured at 620 nm using a plate reader. IRF-dependent Lucia luciferase activity was quantified using the QuantiLuc Solution and luminescence was measured using a plate reader.

**Cytokine quantification.** Following 24 h PBMC stimulation, culture supernatants were collected and transferred to V-bottom plates. After centrifugation at 500 × g for 5 min, supernatants were stored at –

80°C until analysis. Cytokine and chemokine concentrations were determined using LEGENDplex multiplex bead-based assays (BioLegend; Human Inflammation Panel 1) according to the manufacturer's instructions. Samples were measured using a CytoFLEX LX flow cytometer and analyzed using the cloud-based LEGENDplex™ Data Analysis Software Suite (Biolegend).

**Flow cytometry.** Cells were stained with Aqua LIVE/DEAD (Invitrogen) or Live-or-Dye NucFix$^{TM}$Single-stained, fluorescence-minus-one and isotype-matched controls were used for compensation, to define gating boundaries and to assess nonspecific binding. Debris, doublets and non-viable cells were excluded before population identification. Data were analyzed using FlowJo v10.10.1 (BD Biosciences) or FlowLogic v1.4 (Inivai Technologies). T cells were identified as CD3 + CD4+ or CD3 + CD8+, NK cells as CD3 − CD19−CD56+, monocytes as CD3 − CD19−CD56 − CD14+ and macrophages as CD11b + HLA-DR+ cells. Classical, intermediate and non-classical monocytes were defined as CD14 + + CD16−, CD14 + + CD16 + and CD14 + CD16 + + cells, respectively. Used antibody clones are listed in Supplemenatary Table 1.

**NK-mediated Cell Killing Assay.** For the plate-reader assay, target cells were stained with 2 µM Calcein-AM (30 min, 37°C), washed, and resuspended in RPMI with 10% FCS at 8,000 cells/50 µL. Effector cells—isolated NK cells or PBMCs stimulated for 1–3 days with cytokines and immobilized α-CD3 plus soluble α-CD28 antibodies—were co-cultured with target cells in U-bottom 96-well plates at varying effector-to-target (E:T) ratios in 50 µL volumes. Plates were centrifuged at 100 × g for 2 min and incubated at 37°C for 2.5 h. Supernatant fluorescence (485 nm excitation / 535 nm emission) was measured using a Synergy plate reader, and cell death was normalized against six replicates of spontaneous release (no effector cells) and maximum release controls (treated with 1% Triton X-100). For the flow-cytometric assay, target cells were stained with 1 µM CellTrace Violet (20 min, 37°C), neutralized with a 5-fold volume of RPMI with 10% FCS, and adjusted to 30,000 cells/50 µL. Target cells were co-cultured overnight with freshly isolated or rested PBMCs, test compounds, and stimuli. Samples were transferred to V-bottom plates and stained for viability, CD3, CD19, CD56, and CD107a expression. Target cell death was quantified as the percentage of CellTrace Violet and viability dye double-positive cells, whereas NK cell degranulation was assessed as % $CD107a^{+}$ of $CD56^{+}$ $CD3^{-}$ $CD19^{-}$ NK cells.

**Macrophage Differentiation and Polarization.** Monocyte-enriched cell suspensions were seeded in Nunclon Delta tissue-culture-treated plates at $5 \times 10^5$ cells per well in 1 mL medium in 12-well plates or $2.5 \times 10^5$ cells per well in 500 µL medium in 24-well plates. Macrophage differentiation medium consisted of RPMI-1640 supplemented with 1% penicillin/streptomycin, 1% L-glutamine, 10% heat-inactivated fetal calf serum, 10% human AB serum and 15 ng/mL recombinant human M-CSF. Plates were left at room temperature for 10–15 min to allow even settling, and cells were then differentiated for 7 days at 37°C and 5% $CO_2$. On day 3 or 4, the medium was replaced with fresh differentiation medium w/o FCS containing M-CSF and the respective treatments. Where indicated, GPR15LG was present at 5 µM throughout differentiation. Following differentiation, macrophages were polarized for an additional 3 days. M1-associated polarization was induced using 400 U/mL IFN-γ and 100 ng/mL LPS. M2-associated polarization was induced using 20 ng/mL IL-4. Unpolarized M0 controls were maintained for

the same period in macrophage differentiation medium containing M-CSF. Where indicated, GPR15LG was added during the polarization period at a final concentration of 5 µM. Macrophage phenotype was subsequently analyzed by flow cytometry.

**Phagocytosis Assay.** Phagocytosis assay was performed on polarized primary macrophages either in presence or absence of GPR15LG during the polarization step. GPR15LG-treated samples were always exposed to GPR15LG for the duration of the assay. In short, macrophages differentiated from $5 \times 10^5$ cells per 12 well or from $2.5 \times 10^5$ per 24-well were polarized as described above and at the end of the polarization, a full medium change was performed. Cytochalasin was supplied at 1µM concentration for a 20-minute pre-incubation at 37°C prior to the assay start to fully inhibit actin polymerization. The leftover medium (RPMI, 10% human serum, 1% penicillin/streptomycin, 1% L-glutamine, 15 ng/mL M-CSF) with or without 5 µM GPR15LG was carefully dispensed on top of pre-treated macrophages immediately before the beginning of measurement at the IncuCyte instrument. Macrophages were captured with a 20x objective in the brightfield and orange channel every 20 or 30 minutes over a course of 4 hours. Analysis was performed using Incucyte 2024B software. pHrodo-positive objects were quantified with the Basic Analyzer module and macrophage counts and mean macrophage areas with the Adherent Cell-by-Cell Analysis module. The minimum fluorescence intensity threshold was set to the mean intensity of the cytochalasin D-treated control wells at the final time point, and identical segmentation settings were applied to all conditions within an experiment; the complete segmentation parameters are listed in the Supplementary Table 2. Phagocytic activity was expressed as the mean number of pHrodo-positive objects per well, from 9–16 images per well.

**Statistical analysis.** Statistical analyses were performed in GraphPad Prism version 11.0.0 (Massachusetts USA). Each data point represents one independent donor unless stated otherwise. Donor-matched comparisons between two conditions were analysed by paired t test; comparisons involving more than two conditions were analysed by one- or two-way ANOVA with Šídák's or Dunnett's correction for multiple comparisons, as specified in each figure legend. All comparisons involving more than two groups were corrected for multiple testing. Differences were considered significant at $p < 0.05$.

# 3 Results

**GPR15LG enhances CXCL12-directed migration and amplifies immune responses in activated PBMCs.** We previously demonstrated that GPR15LG binds to CXCR4 and synergistically enhances CXCL12-induced signaling and migration of primary CD4 + T cells [9]. To determine whether this effect is maintained after T-cell activation, primary human CD4 + T cells were left unstimulated or activated with antibodies against CD3 and CD28 before migration towards CXCL12 and GPR15LG was assessed. As expected, low doses of CXCL12 had no effect on T cell migration. GPR15LG induced some migration in individual donors, likely reflecting donor-to-donor variability in receptor expression (Fig. 1a, Supplementary Fig. 1). GPR15LG enhanced CXCL12-directed migration of unstimulated T cells with high variation between donors. Although CD3/CD28 stimulation reduced the overall migratory response, GPR15LG significantly increased CXCL12-directed migration of activated T cells (Fig. 1a). Thus,

GPR15LG potentiates CXCL12-dependent T-cell migration in both unstimulated and activated cells under these assay conditions, although absolute migration was lower after activation.

To investigate if GPR15LG also affects T-cell activation, PBMCs were stimulated with increasing concentrations of anti-CD3 antibodies in the presence or absence of GPR15LG. T cells were analyzed by flow cytometry. GPR15LG did not further increase the proportion of CD69 + CD25+ T cells. However, GPR15LG slightly enhanced the stimulation-associated reduction in surface CD3 expression, particularly at lower anti-CD3 concentrations (Fig. 1b, Supplementary Fig. 2). These results suggest that GPR15LG modulates the response to TCR engagement without broadly increasing the expression of conventional T-cell activation markers.

In mixed PBMC populations, activated T cells communicate with other cell types via soluble factors. To examine the functional consequences of GPR15LG during stimulation within the mixed PBMC population, cytokines were quantified in the culture supernatants. GPR15LG alone induced little or no cytokine release and GPR15LG did not reduce cell viability at any concentration tested (Supplementary Fig. 3). In CD3/CD28-stimulated PBMCs, however, GPR15LG significantly increased MCP-1/CCL2, IFN-γ, IFN-α2, IL-18, IL-6, IL-10 and IL-8/CXCL8 concentrations (Fig. 1c). By contrast, IL-1β, TNF-α, IL-33, IL-12p70, IL-17A and IL-23 were not significantly affected. GPR15LG therefore selectively amplified cytokine production initiated by TCR stimulation, including mediators with known effects on innate lymphocytes. Of note, both CXCR4 and GPR15, the two established receptors for GPR15LG, were detectable to varying degrees among the immune-cell populations investigated in this study (Supplementary Fig. 1).

**GPR15LG promotes context-dependent NK-cell activation without enhancing NK-cell migration or cytotoxicity.** Because GPR15LG enhanced the release of cytokines capable of influencing innate immune cells, we next examined NK-cell activation within CD3/CD28-stimulated PBMCs. GPR15LG increased the proportion of CD69 + CD25+ NK cells across a range of anti-CD3 concentrations, with the clearest differences observed at intermediate stimulation strengths (Fig. 2a,b). Titration of GPR15LG further demonstrated a concentration-dependent increase in CD69 + CD25+ NK cells in stimulated, but not unstimulated, PBMCs (Fig. 2c). These findings indicate that GPR15LG enhances NK-cell activation in the context of T-cell stimulation. In addition to CD69 and CD25, GPR15LG concentration-dependently increased endpoint surface CD107a and CD27 expression after prolonged stimulation on NK cells within stimulated PBMCs (Fig. 2d-f). To determine whether GPR15LG acts directly on NK cells or indirectly through release of mediators from other PBMC populations, supernatants from CD3/CD28-stimulated PBMCs cultured with or without GPR15LG were transferred to enriched NK cells. Addition of GPR15LG only during incubation of the enriched NK cells did not reproduce the full activation phenotype observed in PBMC cultures. In contrast, supernatants generated from PBMCs stimulated in the presence of GPR15LG increased CD69 and CD107a expression on enriched NK cells (Fig. 2g-i). Addition of GPR15LG during the second incubation did not substantially enhance this response further. These results indicate that GPR15LG predominantly promotes NK-cell activation indirectly by altering soluble mediators released from stimulated PBMCs.

We next investigated whether GPR15LG could directly modulate NK-cell responses in defined cytokine environments (Supplementary Fig. 4). GPR15LG enhanced IL-12-induced CD69 and CD107a expression in enriched NK cells in a concentration-dependent manner (Supplementary Fig. 4d-g), whereas comparable effects were not observed following stimulation with IL-2, IL-15 or IL-18 alone (Supplementary Fig. 4a-c). GPR15LG also modestly increased CD27 expression on $CD56^{bright}$ NK cells, including in the absence of cytokine stimulation (Supplementary Fig. 5). However, because these preparations contained only 60–80% NK cells, a contribution of residual accessory cells cannot be excluded. Thus, the results identify IL-12 as a permissive cytokine context for GPR15LG-mediated enhancement but do not establish a direct action of GPR15LG on NK cells.

Despite these phenotypic effects, GPR15LG did not further increase CD107a mobilization during co-culture with K562 target cells and did not enhance K562-cell killing. Thus, the GPR15LG-associated increase in steady-state surface CD107a did not translate into enhanced target-cell-induced degranulation or cytotoxicity (Supplementary Fig. 6) Furthermore, GPR15LG did not induce NK cell migration (Supplementary Fig. 7). Collectively, these findings indicate that GPR15LG alters the activation phenotype of NK cells in specific inflammatory environments. Because neither target-cell killing nor degranulation upon target encounter was increased, we describe these changes as a shift in activation phenotype rather than as enhanced NK-cell effector function.

**GPR15LG enhances CD80 expression on human monocytes.** The cytokine-dependent NK-cell response prompted us to examine activation status of other populations within the CD3/CD28 stimulated PBMC cultures. We therefore examined the expression of the co-stimulatory molecule CD80 on monocytes. GPR15LG significantly increased the proportion of CD80 + cells within CD3/CD28 stimulated monocytes, but also within unstimulated monocytes at higher concentrations (Fig. 3a-d). HLA DR presentation was not significantly altered (Supplementary Fig. 8). GPR15LG also increased CD80 expression under LPS stimulation, indicating that the response was not limited to T-cell-driven stimulation conditions (Fig. 3e,f). Analysis of monocyte subsets showed a significant increase among classical monocytes and a comparable but non-significant increase among intermediate monocytes, whereas non-classical monocytes were unaffected (Fig. 3g). These findings identify monocytes as a particularly GPR15LG-responsive population and prompted us to investigate whether GPR15LG also influences longer-term myeloid differentiation and function. Of note, CXCR4 was highly expressed on monocytes and on monocyte-derived macrophages (MDMs), whereas GPR15 was only weakly expressed on a subpopulation of MDMs (Supplementary Fig. 9).

**GPR15LG restricts the acquisition of an M2-associated macrophage phenotype and reduces phagocytic capacity.** GPR15LG is expressed at epithelial barrier tissues and is strongly upregulated under inflammatory conditions, where recruited monocytes differentiate into macrophages and contribute to both the propagation and resolution of inflammation. We therefore examined whether prolonged GPR15LG exposure during macrophage differentiation or polarization alters the resulting cellular phenotype and function. Monocyte-enriched PBMCs were differentiated with M-CSF for seven days in the presence or absence of GPR15LG. Continuous exposure to GPR15LG significantly reduced

the proportion of CD38 + macrophages and produced a similar trend towards reduced CD163 expression (Fig. 4a). Because CD38 and CD163 mark opposing macrophage states, a reduction in both is more consistent with a general attenuation of marker acquisition during M-CSF-driven differentiation than with a shift towards either phenotype. Of note, macrophage viability was unaffected (Supplementary Fig. 10a). To distinguish effects on differentiation from effects during subsequent polarization, monocyte-derived macrophages were first differentiated and then maintained for three additional days as unpolarized M0 controls or exposed to IFN-γ plus LPS (M1-associated conditions) or IL-4 (M2-associated conditions), with or without GPR15LG. We then analyzed CD80 as an inflammatory co-stimulatory marker and CD163 as a scavenger receptor associated with anti-inflammatory and tissue-remodeling macrophages. Under M2-polarizing conditions, GPR15LG markedly reduced the frequency of CD80 – CD163+ macrophages, indicating that GPR15LG interferes with the acquisition or maintenance of this M2-associated surface phenotype (Fig. 4b, Supplementary Fig. 11). The reduction in CD80 – CD163+ macrophages indicates that GPR15LG restricts the acquisition of a phenotype associated with scavenging, tissue remodeling and anti-inflammatory activity. Despite these phenotypic changes, prolonged GPR15LG exposure did not produce consistent changes in macrophage-derived cytokines and chemokines at days 3 or 6 (Supplementary Fig. 12) or lead to reduced cell count or viability (Supplementary Fig. 10b,c).

We next examined whether this phenotypic alteration was accompanied by a functional change. Macrophages exposed to GPR15LG during M2 polarization showed a pronounced reduction in the uptake of fluorescent particles, whereas phagocytosis by M1-polarized macrophages was not significantly affected (Fig. 4c-e). Comparable macrophage numbers and cell areas across the relevant conditions indicated that reduced particle counts were not caused by fewer or smaller macrophages (Supplementary Fig. 13). Cytochalasin D almost completely prevented particle uptake, confirming that the measured signal reflected actin-dependent internalization. To determine whether GPR15LG directly inhibits the phagocytic process, the peptide was added only after macrophage differentiation and polarization, during the phagocytosis assay. Under these conditions, GPR15LG did not significantly affect particle uptake by either M1- or M2-polarized macrophages (Fig. 4f,g). Therefore, the reduced phagocytic capacity observed after exposure during M2 polarization is not caused by acute inhibition of particle uptake but instead reflects a GPR15LG-induced alteration of the functional state acquired during polarization. Because the phenotype was defined using CD38, CD80 and CD163 only, these data document a restricted change rather than a comprehensive repolarization.

**Full-length GPR15LG potentiates TLR-dependent immune-cell activation.** To identify structural and signaling requirements for the immunomodulatory activity of GPR15LG, we first compared full-length GPR15LG with peptides corresponding to its N-terminal amino acids 25–41 and C-terminal amino acids 58–84 (Fig. 5a). The N-terminal fragment binds to CXCR4 [9], whereas the C-terminal fragment is an agonist of GPR15 [16]. PBMCs were stimulated with increasing concentrations of anti-CD3 in the presence of full-length GPR15LG or either peptide fragment. Full-length GPR15LG increased the proportion of CD69 + CD25+ cells among CD3 – CD19– cells and NK cells, as expected. By contrast, neither the N-terminal nor the C-terminal fragment reproduced the activity of the full-length peptide

(Fig. 5b–c). Increasing concentrations of either fragment also failed to block the effect of the full-length peptide (Fig. 5d,e). The immunomodulatory effect of GPR15LG could therefore not be assigned to either isolated terminal region and appeared to require the intact protein.

Because monocytes emerged as a prominent GPR15LG-responsive population, we next investigated whether GPR15LG cooperates with defined innate immune-receptor pathways. THP-1 cells were stimulated with independently titrated agonists of TLR1/2, TLR7/8 or TLR4 in the presence or absence of GPR15LG, and activation was assessed by CD80 surface expression (Fig. 5f-j). GPR15LG markedly enhanced LPS-induced CD80 expression after 24 h, particularly at submaximal LPS concentrations (Fig. 5h). A smaller enhancement was observed at the highest concentration of the TLR1/2 agonist PAM3CSK4, whereas GPR15LG did not detectably affect activation induced by the TLR7/8 agonist R848 (Fig. 5f,g). The interaction with LPS was most apparent after 24 h and was not consistently detected after 48 or 72 h, indicating that the magnitude of the effect depended on both stimulus strength and duration (Fig. 5h–j). To confirm the TLR-dependent effect, CD3/CD28-stimulated PBMCs were treated with increasing concentrations of a TLR2 or TLR4 antagonist. Pharmacological inhibition attenuated the GPR15LG-associated increase in CD80 expression, with the clearest effect observed following TLR4 inhibition (Fig. 5k,l). Because the antagonists also reduced activation in the absence of GPR15LG, these results indicate that intact TLR signaling contributes to the enhancing effect but do not establish direct activation of either receptor by GPR15LG.

We subsequently used THP1-Dual reporter cells to determine whether GPR15LG enhances signaling downstream of TLR4. LPS induced concentration-dependent NF-κB/AP-1 reporter activity, which was significantly increased by GPR15LG at all tested LPS concentrations (Fig. 5m). GPR15LG did not increase the LPS-induced IRF reporter response (Fig. 5n). The immunomodulatory activity of GPR15LG therefore required the full-length peptide, and the strongest interaction was with LPS, where it was accompanied by increased NF-κB/AP-1 reporter activity in intact cells.

# 4 Discussion

Our study extends the biological role of GPR15LG from epithelial homeostasis and GPR15-dependent lymphocyte homing to the regulation of immune-cell activation and function. Across lymphoid and myeloid systems one pattern recurred: GPR15LG showed little activity as an isolated stimulus but substantially modified responses elicited by other signals, including CXCL12, TCR engagement, IL-12 and TLR ligands. Rather than behaving as a conventional pro-inflammatory cytokine, GPR15LG therefore appears to act as a local amplifier and modifier of ongoing immune responses. This is consistent with the broader picture that GPR15LG exerts important functions beyond its canonical receptor, including GPR15-independent effects on epithelial proliferation, barrier regeneration and colitis susceptibility [7, 8, 17].

Two levels of regulation emerged. First, GPR15LG enhanced CXCL12-directed migration not only of resting but also of activated CD4 + T cells, indicating that its modulation of the CXCL12–CXCR4 axis [9]

is maintained across T-cell activation states. In an inflamed tissue this may influence the positioning and retention of infiltrating cells within CXCL12-rich microenvironments rather than only their initial recruitment. Second, within stimulated PBMCs GPR15LG selectively increased IFN-γ, IFN-α2, IL-18, CCL2/MCP-1, IL-6, CXCL8/IL-8 and IL-10 while leaving IL-1β, TNF-α, IL-12p70, IL-17A, IL-23 and IL-33 unchanged. The absence of a broad increase argues against nonspecific activation and instead indicates a targeted reshaping of the inflammatory milieu generated by cellular activation. Several of the enhanced mediators connect directly to downstream innate responses [11, 18–20], whereas the concomitant rise in IL-10 suggests compensatory regulatory feedback rather than a uniform pro-inflammatory shift [21]. GPR15LG also enhanced the stimulation-associated loss of surface CD3 without increasing conventional activation markers; whether this reflects altered TCR internalization, recycling or degradation remains unresolved.

The NK-cell data illustrate this context dependency, and also its limits. Activation within stimulated PBMCs was largely reproduced by conditioned supernatants, indicating a predominantly indirect, soluble-factor-dependent mechanism, and IL-12 – but not IL-2, IL-15 or IL-18 – provided a permissive context for further enhancement. Because the enriched preparations contained only 60–80% NK cells, a direct action on NK cells cannot be claimed. Importantly, neither target-cell killing nor degranulation upon target encounter was increased. GPR15LG therefore appears to shift the activation threshold and surface phenotype of NK cells without demonstrably enhancing cytotoxic effector function, and the biological significance of this shift remains open.

The most prominent responses occurred within the monocytic lineage. GPR15LG increased monocyte CD80 under CD3/CD28 stimulation, under LPS stimulation and, to a lesser extent, in the absence of an additional stimulus, and experiments in THP-1 cells showed that monocytic cells respond outside the complex PBMC environment. CD80 upregulation indicates a shift towards a more co-stimulatory phenotype but, without CD86 data or functional co-stimulation assays, does not establish enhanced antigen presentation or T-cell priming. Mechanistically, the clearest interaction was with TLR4: GPR15LG potentiated LPS-induced activation and NF-κB/AP-1 reporter activity, and TLR4 blockade attenuated the GPR15LG-associated response, although the antagonist also reduced the underlying LPS response. These data support a contribution of intact TLR4 signaling without indicating that GPR15LG is itself a TLR4 ligand – a distinction that matters physiologically, because barrier tissues continuously encounter microbial products [22–25], while tissue injury releases endogenous danger signals that engage overlapping innate pathways [23–27]. As predicted for a cationic host-defense peptide, GPR15LG engaged this pathway, but with the opposite sign to the usual cathelicidin effect [13, 14]. It potentiated rather than neutralized TLR4 responses, an amplifying mode otherwise described for LL-37–self-DNA complexes acting on TLR9 [15]. GPR15LG is similarly cationic and is co-induced with cathelicidins in inflamed skin, and our observation that it potentiates LPS responses in monocytic cells parallels the reduced LPS-induced cytokine expression in GPR15LG-deficient murine keratinocytes [31, 32]. Modulation of innate danger sensing may therefore represent a function shared across epithelial and immune compartments.

Prolonged exposure extended these effects to macrophage fate. GPR15LG altered the phenotype acquired during M-CSF-driven differentiation and, during IL-4 polarization, reduced the CD80 – CD163+ population and generated macrophages with lower phagocytic capacity, whereas acute exposure of already polarized macrophages did not impair particle uptake. GPR15LG thus appears to imprint the functional state acquired during polarization rather than to inhibit the phagocytic machinery, and the direction of this change parallels the increased CD80 observed in monocytes. CD163-associated populations are generally linked to scavenging, tissue remodeling and resolution-associated functions [33–37], and macrophages adapt continuously to signals in their tissue environment [38–42]. The M1/M2 nomenclature is nevertheless an oversimplification, and single-cell analyses describe a continuum of activation states rather than discrete poles [43, 44]; our marker-based readout therefore documents a restricted redirection rather than a comprehensive repolarization. Because GPR15LG is strongly upregulated in lesional psoriasis and atopic dermatitis and has been linked to impaired barrier programs, inflammatory mediator production and pruritus [3, 8, 16, 31, 45], sustained expression in chronically inflamed skin could simultaneously favor co-stimulatory myeloid phenotypes and limit selected resolution-associated functions within the cytokine, chemokine and danger-signal networks that sustain these lesions [11, 20, 24, 46–49]. Whether GPR15LG shapes macrophage states in vivo remains to be established.

The receptor mediating these effects remains unidentified, and we regard this as the principal open question arising from our data. Both established receptors were detectable on the responsive populations (Supplementary Figs. 1 and 9), but expression does not establish dependency. Neither the GPR15-activating C-terminal fragment nor the CXCR4-binding N-terminal fragment reproduced or antagonized the activity of the full-length peptide [9, 50], which argues against either binding region acting in isolation but does not exclude GPR15 or CXCR4, since the intact molecule may be required for productive engagement. Resolving this will require pharmacological blockade and genetic deletion of both receptors in THP-1 cells and primary monocytes, experiments in purified rather than mixed populations, and an assessment of whether TCR engagement itself alters receptor surface levels. A second caveat concerns concentration. Effects were detectable from 0.1–1 μM in PBMC cultures but required 5 μM in the macrophage and THP-1 experiments, above the range at which chemokines engage their receptors and within that reported for cationic host-defense peptides at epithelial surfaces [14]. Local GPR15LG concentrations in inflamed human tissue have not been quantified, so effects seen only at 5 μM should be interpreted with corresponding caution, and receptor-independent contributions such as direct binding to LPS or to the plasma membrane cannot be formally excluded – although the complete inactivity of the equally cationic terminal fragments argues against a purely charge-driven mechanism.

Further limitations should be noted. Most primary-cell experiments used mixed PBMC cultures, which enabled analysis of intercellular effects but limits attribution of responses to individual cell types, and the cellular sources of the enhanced cytokines remain undefined; THP-1 cells demonstrate responsiveness of the monocytic lineage but do not fully reproduce primary-monocyte biology [51]. Several readouts that would convert phenotype into function were not performed, including NK-cell IFN-γ

production, CD86 expression and T-cell co-stimulation assays, and CD206 staining together with transcriptome-wide profiling of the GPR15LG-imprinted macrophage state. All data were obtained in vitro with cells from healthy donors. Within these limits, our findings support a model in which GPR15LG acts at successive stages of a tissue immune response: cooperating with CXCL12 to influence recruitment and local positioning, then amplifying selected responses to TCR-, cytokine- and pattern-recognition receptor signals, and, upon prolonged exposure, redirecting macrophage polarization and function. GPR15LG may therefore be less an inflammatory mediator in its own right than a local determinant of how immune cells interpret other signals within an inflamed tissue, which could explain why its strong upregulation has substantial biological consequences despite its modest activity in isolation.

## Declarations

# Competing interest.

The authors declare no competing interests.

# Ethics approval and consent to participate.

The use of buffy coats from healthy, anonymized adult blood donors. No approval was needed by the Ethics Committee of Ulm University. All donors provided written informed consent. All experiments were performed in accordance with the Declaration of Helsinki. No animal experiments were performed in this study.

**Consent for publication.**

Not applicable.

# Funding.

M.H. receives funding by the Baden-Württemberg Foundation (Eliteprogramme for Postdocs), by the DFG (project number 585272342) and is supported by the Medical Scientist Program of the Ulm University Medical Centre. M.H. and J.M. are supported by the DFG funded RTG (Org-BOOST). SV receives funding from the DFG (project number 537908488 (VE 994/4 – 1)).

# Author Contribution

SA: Conceptualization, Investigation, Methodology, Validation, Visualization, Formal Analysis, Writing – original draft, review & editing; DA: Conceptualization, Investigation, Methodology, Writing – review & editing; LF: Investigation, Validation, Formal Analysis, Visualization, Writing – review & editing; FK: Investigation, Validation, Formal Analysis, Writing – review & editing; TN: Investigation, Writing – review &

editing; SV: Investigation, Writing – review & editing; JM: Supervision, Funding Acquisition, Resources, Writing – review & editing; MH: Conceptualization, Supervision, Writing – original draft, review & editing, Visualization, Resources, Project Administration, Funding Acquisition, Formal Analysis.

# Data Availability

All data supporting the findings of this study are available within the paper and its Supplementary Information. Raw data are available upon reasonable request.

## References


1. Ocón B, Pan J, Dinh TT, Chen W, Ballet R, Bscheider M, et al. A Mucosal and Cutaneous Chemokine Ligand for the Lymphocyte Chemoattractant Receptor GPR15. Front Immunol. 2017;8:1111. https://doi.org/10.3389/fimmu.2017.01111.
2. Yang M, Tang M, Ma X, Yang L, He J, Peng X, et al. AP-57/C10orf99 is a new type of mutifunctional antimicrobial peptide. Biochem Biophys Res Commun. 2015;457:347–52. https://doi.org/10.1016/j.bbrc.2014.12.115.
3. Chen C, Wu N, Duan Q, Yang H, Wang X, Yang P, et al. C10orf99 contributes to the development of psoriasis by promoting the proliferation of keratinocytes. Sci Rep Nat Publishing Group. 2018;8:8590. https://doi.org/10.1038/s41598-018-26996-z.
4. Suply T, Hannedouche S, Carte N, Li J, Grosshans B, Schaefer M, et al. A natural ligand for the orphan receptor GPR15 modulates lymphocyte recruitment to epithelia. Sci Signal Am Association Advancement Sci. 2017;10:eaal0180. https://doi.org/10.1126/scisignal.aal0180.
5. Smith PM, Howitt MR, Panikov N, Michaud M, Gallini CA, Bohlooly-Y M, et al. The microbial metabolites, short chain fatty acids, regulate colonic Treg cell homeostasis. Science. 2013;341. 10.1126/science.1241165.
6. Lahl K, Sweere J, Pan J, Butcher E. Orphan chemoattractant receptor GPR15 mediates dendritic epidermal T-cell recruitment to the skin. Eur J Immunol. 2014;44:2577–81. https://doi.org/10.1002/eji.201444628.
7. Sezin T, Kempen L, Meyne L-M, Mousavi S, Zillikens D, Sadik CD. GPR15 is not critically involved in the regulation of murine psoriasiform dermatitis. J Dermatol Sci. 2019;94:196–204. https://doi.org/10.1016/j.jdermsci.2019.01.008.
8. Tseng P-Y, Hoon MA. GPR15L is an epithelial inflammation-derived pruritogen. Sci Adv. 2022;8:eabm7342. https://doi.org/10.1126/sciadv.abm7342.
9. Albers DPJ, Novikova S, Vieyto-Nuñez J, Almeida-Hernández Y, Pastorio C, Klassen F, et al. GPR15LG binds CXCR4 and synergistically modulates CXCL12-induced cell signaling and migration. Cell Commun Signal. 2025;23:234. https://doi.org/10.1186/s12964-025-02231-x.

10. Farnsworth RH, Karnezis T, Maciburko SJ, Mueller SN, Stacker SA. The Interplay Between Lymphatic Vessels and Chemokines. Front Immunol. 2019;10:518. https://doi.org/10.3389/fimmu.2019.00518.
11. Zhang L, Type. 1 Interferons Potential Initiating Factors Linking Skin Wounds With Psoriasis Pathogenesis. Front Immunol [Internet]. Frontiers; 2019 [cited 2026 Sept 14];10. https://doi.org/10.3389/fimmu.2019.01440.
12. Narayanan D, Sim SL, Kumari S. Skin immunity and inflammation: cellular interactions and communication. Clin Transl Immunol. 2025;14:e70053. https://doi.org/10.1002/cti2.70053.
13. Mookherjee N, Brown KL, Bowdish DME, Doria S, Falsafi R, Hokamp K et al. Modulation of the TLR-mediated inflammatory response by the endogenous human host defense peptide LL-37. J Immunol. Baltimore, Md.: 1950; 2006;176:2455–64. https://doi.org/10.4049/jimmunol.176.4.2455
14. Scheenstra MR, van Harten RM, Veldhuizen EJA, Haagsman HP, Coorens M. Cathelicidins Modulate TLR-Activation and Inflammation. Front Immunol. 2020;11. https://doi.org/10.3389/fimmu.2020.01137.
15. Lande R, Gregorio J, Facchinetti V, Chatterjee B, Wang Y-H, Homey B, et al. Plasmacytoid dendritic cells sense self-DNA coupled with antimicrobial peptide. Nature. 2007;449:564–9. https://doi.org/10.1038/nature06116.
16. Ocón B, Pan J, Dinh TT, Chen W, Ballet R, Bscheider M, et al. A Mucosal and Cutaneous Chemokine Ligand for the Lymphocyte Chemoattractant Receptor GPR15. Front Immunol [Internet]. Front Media SA. 2017. https://doi.org/10.3389/fimmu.2017.01111. [cited 2024 July 4];8.
17. O'Connor GJ, Wigmore RM, Van NT, Choi JC, Zhang K, Kivolowitz C, et al. C10ORF99 (GPR15L) increases susceptibility to colitis and colitis-induced colorectal cancer via GPR15-independent mechanisms, while mediating GPR15-dependent T cell migration to the large intestine. Mucosal Immunol. 2025;18:1229–39. https://doi.org/10.1016/j.mucimm.2025.08.001.
18. Novoszel P, Holcmann M, Stulnig G, De Sa Fernandes C, Zyulina V, Borek I, et al. Psoriatic skin inflammation is promoted by c-Jun/AP-1-dependent CCL2 and IL-23 expression in dendritic cells. EMBO Mol Med. 2021;13:e12409. https://doi.org/10.15252/emmm.202012409.
19. Mohamed Attia HR, Mikhael N, Ismail S. Interleukin-18 expression and the response to treatment in patients with psoriasis. Arch Med Sci AMS. 2010;6:964–70. https://doi.org/10.5114/aoms.2010.19309.
20. Purzycka-Bohdan D, Nedoszytko B, Zabłotna M, Gleń J, Szczerkowska-Dobosz A, Nowicki RJ. Chemokine Profile in Psoriasis Patients in Correlation with Disease Severity and Pruritus. Int J Mol Sci Multidisciplinary Digit Publishing Inst. 2022;23:13330. https://doi.org/10.3390/ijms232113330.
21. Asadullah K, Sterry W, Stephanek K, Jasulaitis D, Leupold M, Audring H, et al. IL-10 is a key cytokine in psoriasis. Proof of principle by IL-10 therapy: a new therapeutic approach. J Clin Invest. 1998;101:783–94. https://doi.org/10.1172/JCI1476.
22. Panzer R, Blobel C, Fölster-Holst R, Proksch E. TLR2 and TLR4 expression in atopic dermatitis, contact dermatitis and psoriasis. Exp Dermatol. 2014;23:364–6. https://doi.org/10.1111/exd.12383.

23. Begon E, Michel L, Flageul B, Beaudoin I, Jean-Louis F, Bachelez H, et al. Expression, subcellular localization and cytokinic modulation of Toll-like receptors (TLRs) in normal human keratinocytes: TLR2 up-regulation in psoriatic skin. Eur J Dermatol EJD. 2007;17:497–506. https://doi.org/10.1684/ejd.2007.0264.
24. Lai C-Y, Su Y-W, Lin K-I, Hsu L-C, Chuang T-H. Natural Modulators of Endosomal Toll-Like Receptor-Mediated Psoriatic Skin Inflammation. J Immunol Res. 2017;2017:7807313. https://doi.org/10.1155/2017/7807313.
25. Yimin, Kohanawa M, Zhao S, Ozaki M, Haga S, Nan G, et al. Contribution of Toll-Like Receptor 2 to the Innate Response against Staphylococcus aureus Infection in Mice. PLoS ONE. 2013;8:e74287. https://doi.org/10.1371/journal.pone.0074287.
26. Clarke TB, Francella N, Huegel A, Weiser JN. Invasive Bacterial Pathogens Exploit TLR-Mediated Downregulation of Tight Junction Components to Facilitate Translocation across the Epithelium. Cell Host Microbe. 2011;9:404–14. https://doi.org/10.1016/j.chom.2011.04.012.
27. Semin I, Ninnemann J, Bondareva M, Gimaev I, Kruglov AA. Interplay Between Microbiota, Toll-Like Receptors and Cytokines for the Maintenance of Epithelial Barrier Integrity. Front Med [Internet] Front. 2021. https://doi.org/10.3389/fmed.2021.644333. [cited 2026 Sept 16];8.
28. Sun N, Ogulur I, Mitamura Y, Yazici D, Pat Y, Bu X, et al. The epithelial barrier theory and its associated diseases. Allergy. 2024;79:3192–237. https://doi.org/10.1111/all.16318.
29. Liu T, Zhang L, Joo D, Sun S-C. NF-κB signaling in inflammation. Signal Transduct Target Ther. Nat Publishing Group. 2017;2:17023. https://doi.org/10.1038/sigtrans.2017.23.
30. Ferrara F, Valacchi G. Role of microbiota in the GUT-SKIN AXIS responses to outdoor stressors. Free Radic Biol Med. 2024;225:894–909. https://doi.org/10.1016/j.freeradbiomed.2024.11.003.
31. Dainichi T, Nakano Y, Doi H, Nakamizo S, Nakajima S, Matsumoto R, et al. C10orf99/GPR15L Regulates Proinflammatory Response of Keratinocytes and Barrier Formation of the Skin. Front Immunol [Internet] Front. 2022. https://doi.org/10.3389/fimmu.2022.825032. [cited 2025 June 17];13.
32. Chen C, Cai R, Zhou J, Zhang D, Chen L. GPR15LG regulates psoriasis-like inflammation by down-regulating inflammatory factors on keratinocytes. Biosci Rep. 2024;44:BSR20231347. https://doi.org/10.1042/BSR20231347.
33. Alshihmani AHH, Mahmoudi M, Kheder RK, Fadaee A, Esmaeili S. The M2 Macrophages Importance Role in Psoriasis. Immun Inflamm Dis. 2025;13:e70211. https://doi.org/10.1002/iid3.70211.
34. Fuchs A-K, Syrovets T, Haas KA, Loos C, Musyanovych A, Mailänder V, et al. Carboxyl- and amino-functionalized polystyrene nanoparticles differentially affect the polarization profile of M1 and M2 macrophage subsets. Biomaterials. 2016;85:78–87. https://doi.org/10.1016/j.biomaterials.2016.01.064.
35. Kristiansen M, Graversen JH, Jacobsen C, Sonne O, Hoffman HJ, Law SK, et al. Identification of the haemoglobin scavenger receptor. Nature. 2001;409:198–201. https://doi.org/10.1038/35051594.

36. Mantovani A, Marchesi F, Malesci A, Laghi L, Allavena P. Tumor-Associated Macrophages as Treatment Targets in Oncology. Nat Rev Clin Oncol. 2017;14:399–416. https://doi.org/10.1038/nrclinonc.2016.217.
37. Etzerodt A, Moestrup SK. CD163 and inflammation: biological, diagnostic, and therapeutic aspects. Antioxid Redox Signal. 2013;18:2352–63. https://doi.org/10.1089/ars.2012.4834.
38. Heinsbroek SEM, Taylor PR, Martinez FO, Martinez-Pomares L, Brown GD, Gordon S. Stage-Specific Sampling by Pattern Recognition Receptors during Candida albicans Phagocytosis. PLoS Pathog. 2008;4:e1000218. https://doi.org/10.1371/journal.ppat.1000218.
39. Wu X, Wang Z, Shi J, Yu X, Li C, Liu J, et al. Macrophage polarization toward M1 phenotype through NF-κB signaling in patients with Behçet's disease. Arthritis Res Ther. 2022;24:249. https://doi.org/10.1186/s13075-022-02938-z.
40. Yunna C, Mengru H, Lei W, Weidong C. Macrophage M1/M2 polarization. Eur J Pharmacol. 2020;877:173090. https://doi.org/10.1016/j.ejphar.2020.173090.
41. Gu S, Xu L, Huang B, Xiong K, Yang X, Ye J. Decoding Macrophage Dynamics: A Pathway to Understanding and Treating Inflammatory Skin Diseases. Int J Mol Sci. 2025;26:4287. https://doi.org/10.3390/ijms26094287.
42. Falda A. Macrophage Plasticity: Phenotypic and Functional Profiles Across Pathological Microenvironments. Int J Mol Sci Multidisciplinary Digit Publishing Inst. 2026;27:5333. https://doi.org/10.3390/ijms27125333.
43. Mulder K, Patel AA, Kong WT, Piot C, Halitzki E, Dunsmore G, et al. Cross-tissue single-cell landscape of human monocytes and macrophages in health and disease. Immunity. 2021;54:1883–e1900. https://doi.org/10.1016/j.immuni.2021.07.007. 5.
44. Sanin DE, Ge Y, Marinkovic E, Kabat AM, Castoldi A, Caputa G, et al. A common framework of monocyte-derived macrophage activation. Sci Immunol. 2022;7:eabl7482. https://doi.org/10.1126/sciimmunol.abl7482.
45. Chen C, Ye Z. C10orf99 regulates angiogenesis by regulating VEGF and MMP2 in psoriasis. Skin Res Technol. 2024;30:e13819. https://doi.org/10.1111/srt.13819.
46. Morizane S, Yamasaki K, Mühleisen B, Kotol PF, Murakami M, Aoyama Y, et al. Cathelicidin antimicrobial peptide LL-37 in psoriasis enables keratinocyte reactivity against TLR9 ligands. J Invest Dermatol. 2012;132:135–43. https://doi.org/10.1038/jid.2011.259.
47. Powles AV, Baker BS, Rutman AJ, McFadden JP, Valdimarsson H, Fry L. Epidermal rupture is the initiating factor for the Koebner response in psoriasis. Acta Derm Venereol. 1990;70:35–8.
48. Kaburagi Y, Shimada Y, Nagaoka T, Hasegawa M, Takehara K, Sato S. Enhanced production of CC-chemokines (RANTES, MCP-1, MIP-1α, MIP-1β, and eotaxin) in patients with atopic dermatitis. Arch Dermatol Res. 2001;293:350–5. https://doi.org/10.1007/s004030100230.
49. Abdelaal NH, Elhefnawy NG, Abdulmonem SR, Sayed S, Saleh NA, Saleh MA. Evaluation of the expression of the stromal cell-derived factor-1 alpha (CXCL 12) in psoriatic patients after treatment with Methotrexate. J Cosmet Dermatol. 2020;19:253–8. https://doi.org/10.1111/jocd.12994.

50. Deng Y, Perez Almeria CV, van Gijzel L, Schaller K, Vedel L, Gloriam DE, et al. Structure–activity relationship of GPR15L peptide analogues and investigation of their interaction with the GPR15 receptor. Basic Clin Pharmacol Toxicol. 2023;132:459–71. https://doi.org/10.1111/bcpt.13861.

51. Forrester MA, Wassall HJ, Hall LS, Cao H, Wilson HM, Barker RN, et al. Similarities and differences in surface receptor expression by THP-1 monocytes and differentiated macrophages polarized using seven different conditioning regimens. Cell Immunol. 2018;332:58–76. https://doi.org/10.1016/j.cellimm.2018.07.008.

# Figures

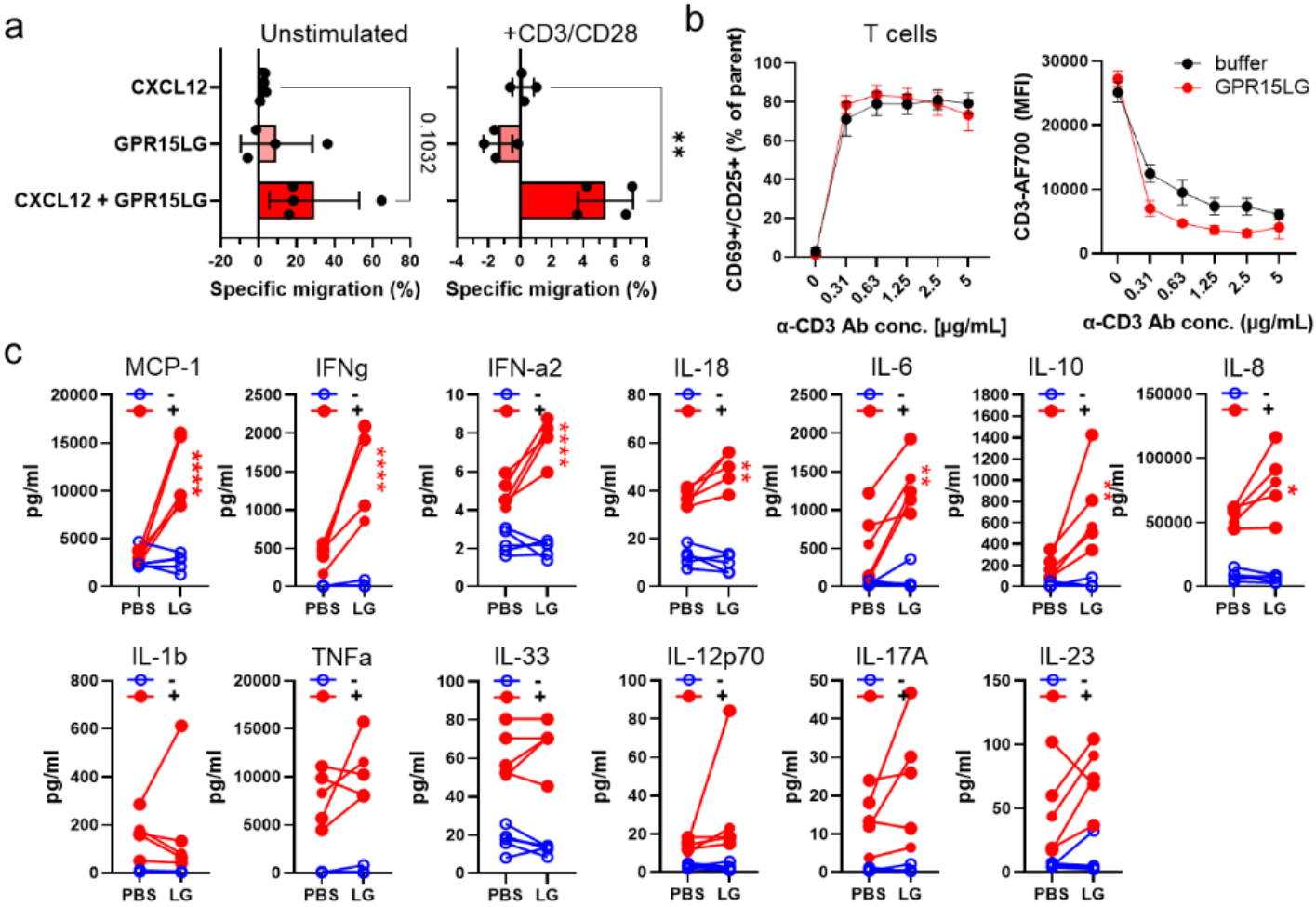



**Figure 1**

**GPR15LG enhances T cell migration and cytokine release from PBMCs, but not T cell stimulation.** a) GPR15LG enhances CXCL12-directed T cell migration. Primary CD4+ T cells were allowed to migrate towards 10 ng/ml CXCL12 alone or in combination with 500 nM GPR15LG in a transwell migration plate. n=4 donors ±SEM. **p<0.01 (one-way ANOVA with Šídák's multiple comparisons test) b) GPR15LG enhances stimulation-associated downregulation of surface CD3 without increasing conventional T-cell activation markers. n = 6 ±SEM. (two-way ANOVA with Tukey's multiple comparisons test). c) GPR15LG

enhances cytokine release from PBMCs during stimulation. PBMCs were stimulated with CD3/CD28 for 24h in absence and presence of 1 µM GPR15LG and supernatants analyzed with LEGENDPlex. n = 4-6 donors. *p<0.05; **p<0.01; ***p<0.001; ****p<0.0001 (two-way ANOVA with Šídák's multiple comparisons test). LG = GPR15LG

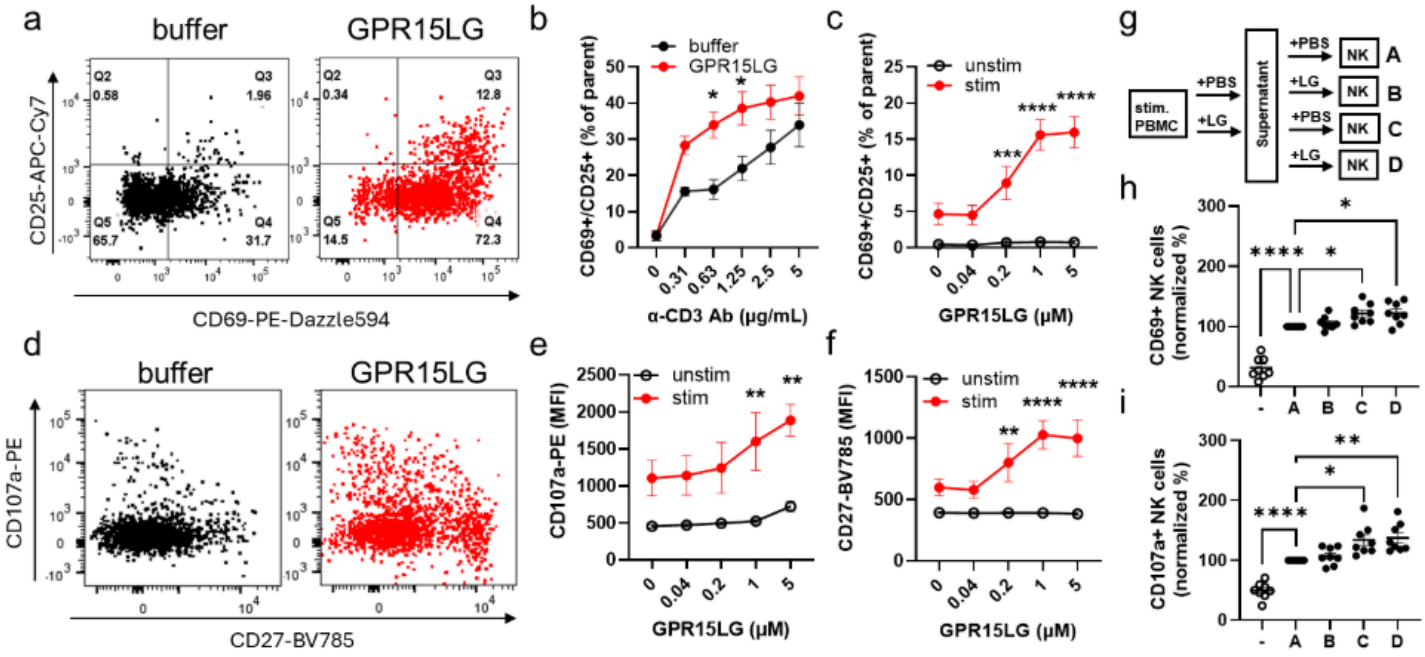
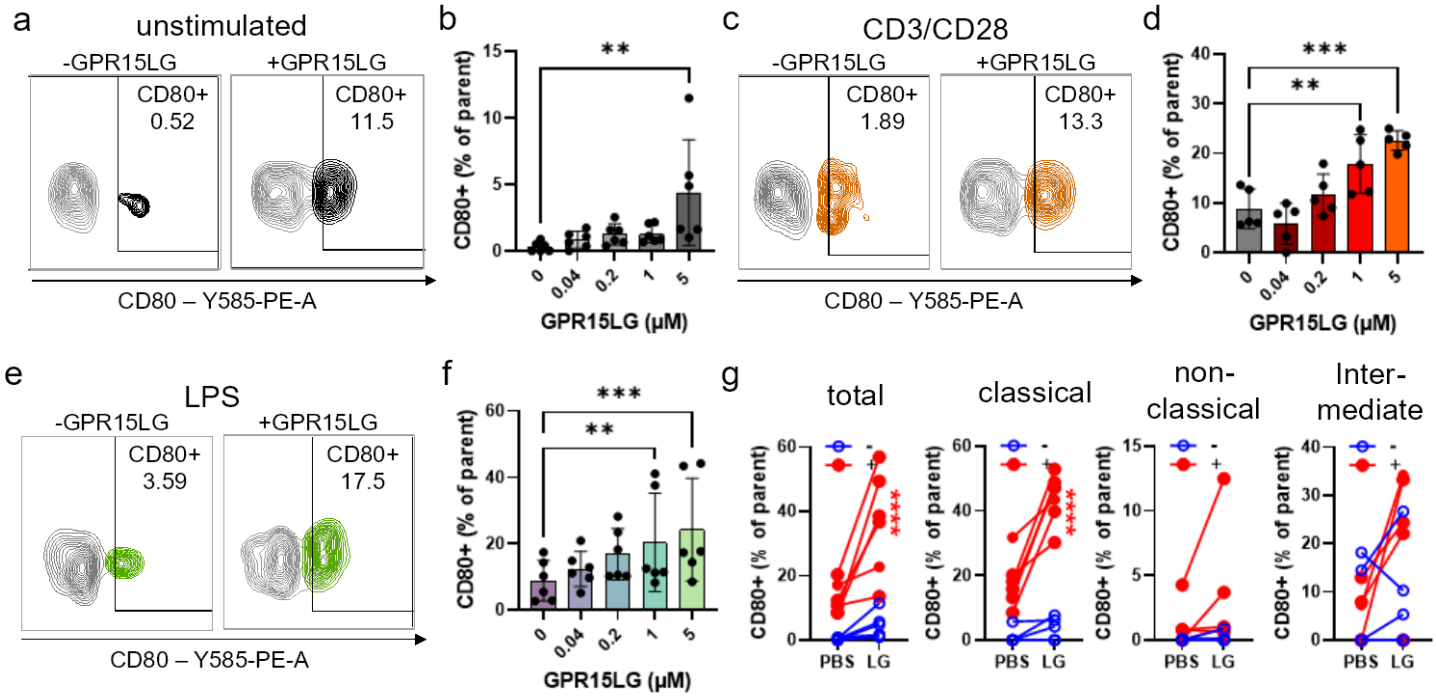



**Figure 2**

**GPR15LG indirectly enhances NK cell activation in CD3/CD28 stimulated PBMCs.** a-f) PBMCs were activated with α-CD3/α-CD28 antibodies in presence of GPR15LG. After 24 h, NK cells within the mixture were analyzed for activation marker expression in flow cytometry. n = 6 donors ±SEM. a, d) Primary dot plots of NK cells from one representative donor stimulated with 5 µg/ml α-CD3 and 1 µM GPR15LG. b) different α-CD3 antibody concentrations were used for stimulation in presence of 1 µM GPR15LG. c, e, f) PBMCs were stimulated with 0.625 µg/ml α-CD3 in the presence of different GPR15LG concentrations. *p<0.05; **p<0.01; ***p<0.001; ****p<0.0001 (two-way ANOVA with Šídák's multiple comparisons test). g-i) Supernatant transfer experiment. PBMCs were stimulated in the presence or absence of 1 µM GPR15LG for 24h. The supernatant was then used to further activate isolated NK cells in the presence and absence of 1 µM GPR15LG for 24h. NK cells were then analyzed for activation marker expression in flow cytometry. - = no activation; A = no GPR15LG during PBMC and NK cell activation; B = GPR15LG was only present during NK cell activation; C = GPR15LG was only present during PBMC activation; D = GPR15LG was present during NK and PBMC activation. A schematic presentation of the assay is shown in (g). n = 8 donors ±SEM. *p<0.05; **p<0.01; ***p<0.001; ****p<0.0001 (one-way ANOVA with Dunnett's multiple comparisons test). LG = GPR15LG




## Figure 3

**GPR15LG enhances monocyte activation.** a-f) PBMCs were left unstimulated (a,b) stimulated with α-CD3/α-CD28 antibodies (c,d), or LPS (e,f) in the presence of indicated concentrations of GPR15LG for 24 h. Monocytes were analyzed via flow cytometry. a,c,e) Representative flow cytometry plots (GPR15LG = 1 µM). b,d,f) Percentage of $CD80^+$ monocytes. n = 5-6 donors ± SEM. *p<0.05; **p<0.01; ***p<0.001; ****p<0.0001 (one-way ANOVA with Dunnett's multiple comparisons test). g) $CD80^+$ cells within the different monocyte subtypes. Cells were stimulated with α-CD3/CD28 antibodies as described above (GPR15LG = 5µM) Shown are total monocates, classical (CD14+CD16-), non-classical (CD14dimCD16+), and intermediate (CD14+CD16+) monocytes. Unstimulated samples are plotted in blue, α-CD3/CD28 stimulated samples in red. n = 3-6 donors ±SEM. *p<0.05; **p<0.01; ***p<0.001; ****p<0.0001 (two-way ANOVA with Šídák's multiple comparisons test). LG = GPR15LG

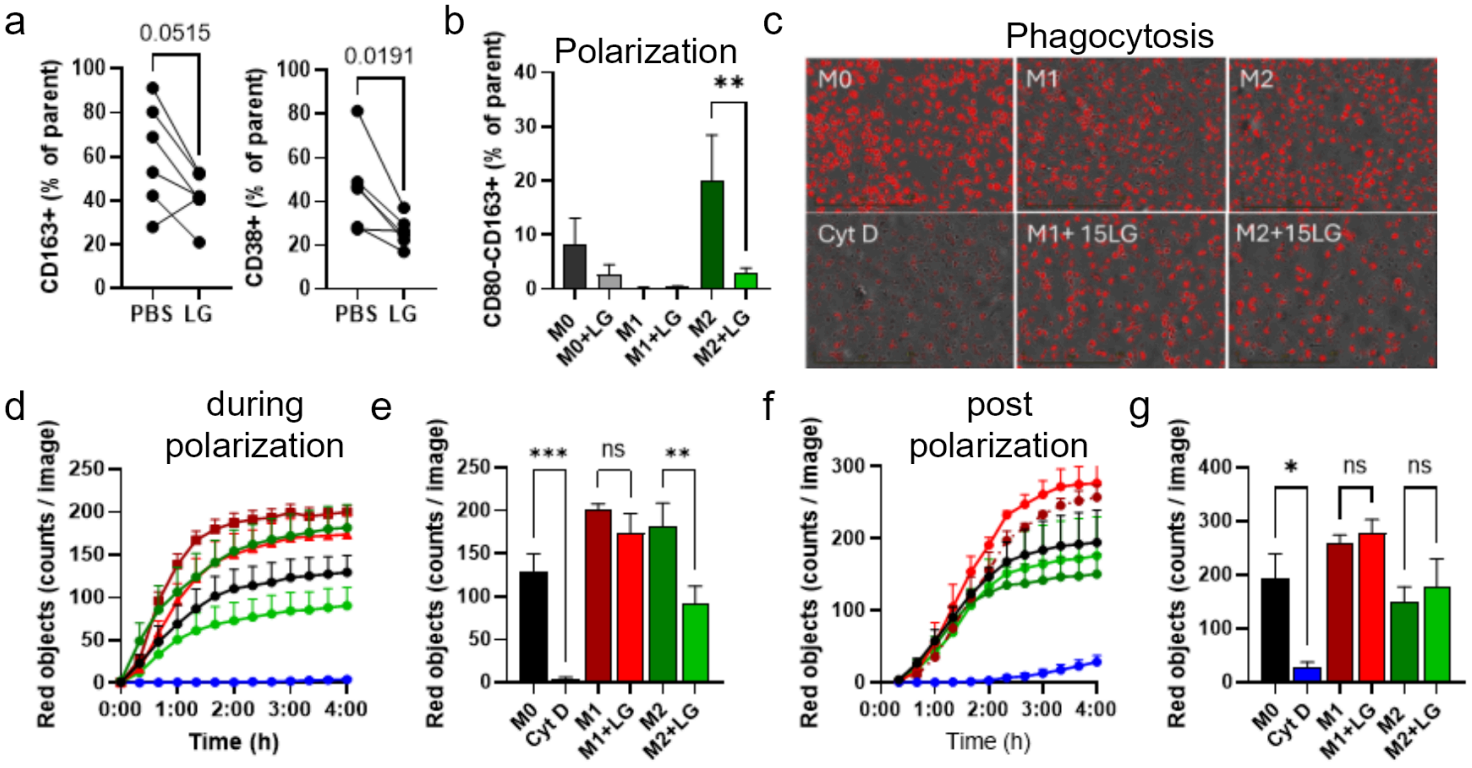
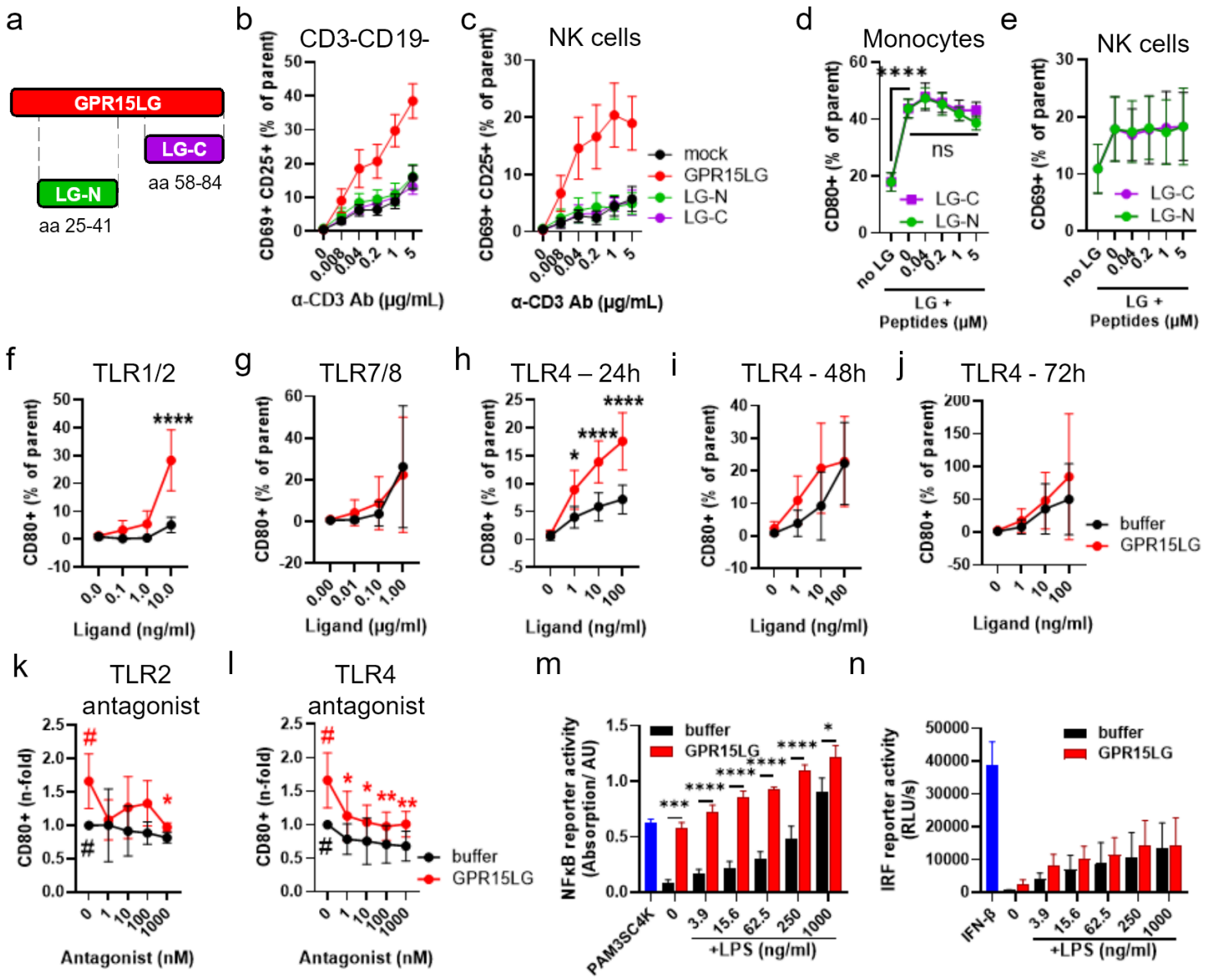



**Figure 4**

**GPR15LG restricts M2-associated phenotype and yields macrophages with reduced phagocytic capacity.** a) GPR15LG impairs PBMC-derived macrophage differentiation. PBMCs were differentiated with M-CSF for 7 days in the presence or absence of 5 µM GPR15LG. Surface markers were analyzed by flow cytometry. (n = 6, Statistics: paired t test) b) GPR15LG suppresses M2-marker expression when applied during polarization. Monocyte-derived MDMs were polarized under M0-, M1-, or M2 conditions in the presence and absence of 5 µM GPR15LG for 3 days. Surface markers were analyzed in flow cytometry. n = 5-6 ± SEM. c-e) GPR15LG-polarized primary M2 macrophages show lower phagocytic capacity compared to control M2 macrophages. c) Representative microscopy images of one donor. d) Quantification for individual time points. e) Endpoint quantification. f-g) Addition of 5 µM GPR15LG to fully differentiated and polarized M1 or M2 macrophages for the duration of the phagocytosis assay did not reduce phagocytosis. n=3-6 donors ± SEM. b,e,f) ns=not significant; *p<0.05; **p<0.01; ***p<0.001; ****p<0.0001 (one-way ANOVA with Šídák's multiple comparisons test). LG = GPR15LG




## Figure 5

**Full-length GPR15LG potentiates TLR-dependent activation and enhances LPS-induced signaling.** a) N- and C-terminal fragments of GPR15LG. b-c) PBMCs were stimulated with α-CD3/α-CD28 antibodies in the presence of 1 μM of full length GPR15LG, or C-terminal or N-terminal fragments for 24 h. Cells were analyzed for activation markers in flow cytometry. n = 6 ± SEMs. d-e) Increasing concentrations of terminal GPR15LG fragments were added to CD3/CD28 stimulated PBMCs in combination with 1 μM full length peptide. Cells were analyzed for activation markers in flow cytometry. n = 6 ± SEMs. f-j) THP-1 cells were stimulated with different TLR agonists in the presence or absence of 5 μM GPR15LG for 24-72 h. Means of n = 3 experiments performed in duplicate ± SEMs are shown. k-l) PBMCs were stimulated with α-CD3/α-CD28 in presence or absence of 1 μM GPR15LG and with increasing concentrations of indicated TLR antagonists: MMG-11 as a TLR2 antagonist and resatorvid as a TLR4 antagonist. Cells were analyzed in flow cytometry for activation. n = 4 ± SEMs. m-n) THP-1 dual reporter IRF/ NFkB cells were stimulated with rising LPS concentration with or without 5μM GPR15LG for 24 hours; NFkB

pathway induction was detected via secreted embryonic alkaline phosphatase (SEAP) activity (m) and IRF induction via Lucia luciferase activity measurement (n); means of n=4 experiments performed in triplicates shown, ± SEMs. b-j and m-n) *p<0.05; **p<0.01; ***p<0.001; ****p<0.0001 (two-way ANOVA with Šídák's multiple comparisons test). k-l) *p<0.05; **p<0.01; ***p<0.001; ****p<0.0001 (two-way ANOVA with Dunnett's multiple comparisons test, Values were compared to #, respectively). LG = GPR15LG, LG-N = N-terminal GPR15LG fragment, LG-C = C-terminal GPR15LG fragment.

## Supplementary Files

This is a list of supplementary files associated with this preprint. Click to download.

- 261023Supplement1Albers.pdf
- 260916Supplement2Albers.pdf